Panchromatic Sensitizers

DOI: 10.1002/anie.201305975

Highly Efficient Dye-Sensitized Solar Cells Based on Panchromatic Ruthenium Sensitizers with Quinolinylbipyridine Anchors

Chun-Cheng Chou, Fa-Chun Hu, Hsiu-Hsuan Yeh, Hsin-Pei Wu, Yun Chi, John N. Clifford,* Emilio Palomares, Shih-Hung Liu, Pi-Tai Chou,* and Gene-Hsiang Lee*

Abstract: *Panchromatic Ru^{II} sensitizers TF-30–TF-33 bearing a new class of 6-quinolin-8-yl-2,2′-bipyridine anchor were synthesized and tested under AM1.5 G simulated solar irradiation. Their increased π conjugation relative to that of the traditional 2,2′:6′,2″-terpyridine-based anchor led to a remarkable improvement in absorptivity across the whole UV–Vis–NIR spectral regime. Furthermore, the introduction of a bulky tert-butyl substituent on the quinolinyl fragment not only led to an increase in the J_{SC} value owing to the suppression of dye aggregation, but remarkably also resulted in no loss in V_{OC} in comparison with the reference sensitizer containing a tricarboxyterpyridine anchor. The champion sensitizer in DSC devices was found to be TF-32 with a performance of J_{SC} = 19.2 mA cm^{-2}, V_{OC} = 740 mV, FF = 0.72, and η = 10.19 %. This 6-quinolin-8-yl-2,2′-bipyridine anchor thus serves as a prototype for the next generation of Ru^{II} sensitizers with any tridentate ancillary.*

The establishment of a low-carbon society requires emerging renewable energy sources, for which third-generation photovoltaic technology, such as dye-sensitized solar cells, is considered to be one of the best candidates.[1] To date, ruthenium(II)-based sensitizers, such as $\{(C_4H_9)_4N\}_2[Ru(Hdcbpy)_2(NCS)_2]$ (N719; dcbpy = 4,4′-dicarboxy-2,2′-bipyridine), $\{(C_4H_9)_4N\}_3[Ru(Htctpy)(NCS)_3]$ (black dye or N749; tctpy = 4,4′,4″-tricarboxy-2,2′:6′,2″-terpyridine),[2] and functionalized derivatives,[3] have received the greatest amount of academic and industrial attention, and have exhibited conversion efficiencies among the highest reported for sensitizers with optimal device stability. However, for practical use, the current records of device efficiency still must be improved upon; better sensitizers are therefore urgently needed to push forward the frontiers of this field of research.[4] Naturally, ingenious dye design is required for maximizing the conversion efficiency (η), the short-circuit current (J_{SC}), and the open-circuit voltage (V_{OC}).[5] To overcome this challenge, panchromatic sensitizers are needed with high absorptivity extending well into the near-infrared (NIR) regime to harvest a wider coverage of solar irradiation for a higher photocurrent. Simultaneously, sensitizer structures can be modified and cell designs optimized to suppress the dark current and maintain the high open-circuit voltage necessary for outstanding cells.

The fulfillment of all of these goals, however, is far from trivial. In the case of the black dye, the lowest-lying absorption-band maximum is located at 606 nm with a shoulder extending down to approximately 800 nm. These absorptions are assigned to the spin-allowed and spin-forbidden metal-to-ligand charge-transfer transitions, that is, ^{1}MLCT and ^{3}MLCT, respectively.[2a] This and similar dyes generally have inferior absorptivity. As a result, it is necessary to fabricate cells with thicker TiO_2 layers to maximize the short-circuit current. However, this strategy generally results in a trade-off in the form of a lower device voltage V_{OC}.[6] The situation was somewhat improved in a class of thiocyanate-free sensitizers, including TF-1 (Scheme 1), the absorption

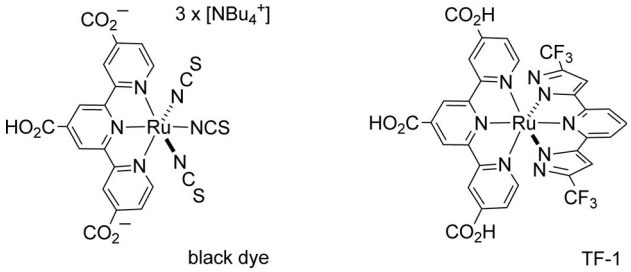

Scheme 1. Structures of black dye and TF-1.

bands of which were slightly more intense in both the higher-energy and NIR regions of the spectrum. However, the absorptivity was unexpectedly low (as compared with that of black dye) in the spectral range of 550 to 700 nm (Figure 1).[7] In this study, with the goal of finding a better molecular design, we turned to the 6-quinolin-8-yl-2,2′-bipyridine anchor, Qbpy, which was expected to show greater chelate π conjugation relative to that of the traditional 2,2′:6′,2″-

[*] C.-C. Chou,[+] F.-C. Hu,[+] H.-H. Yeh, H.-P. Wu, Y. Chi
Department of Chemistry and Low Carbon Energy Research Center
National Tsing Hua University
Hsinchu 30013 (Taiwan)
E-mail: ychi@mx.nthu.edu.tw
J. N. Clifford, E. Palomares
Institute of Chemical Research of Catalonia (ICIQ)
Avda. Països Catalans 16, 43007 Tarragona (Spain)
E-mail: jnclifford@iciq.es
E. Palomares
ICREA, Avda. Lluís Companys 28
Barcelona E-08030 (Spain)
S.-H. Liu, P.-T. Chou, G.-H. Lee
Department of Chemistry and Center for Emerging Material and Advanced Devices, National Taiwan University
Taipei 10617 (Taiwan)
E-mail: chop@ntu.edu.tw
[+] These authors contributed equally.

Supporting information for this article is available on the WWW under http://dx.doi.org/10.1002/anie.201305975.

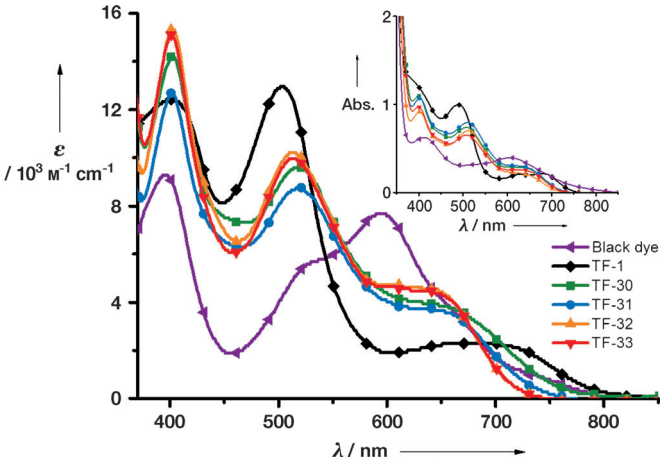

Figure 1. UV/Vis absorption spectra of various Ru^{II} sensitizers in DMF. Inset: spectra of Ru^{II} sensitizers adsorbed on 6 μm transparent TiO_2 thin film.

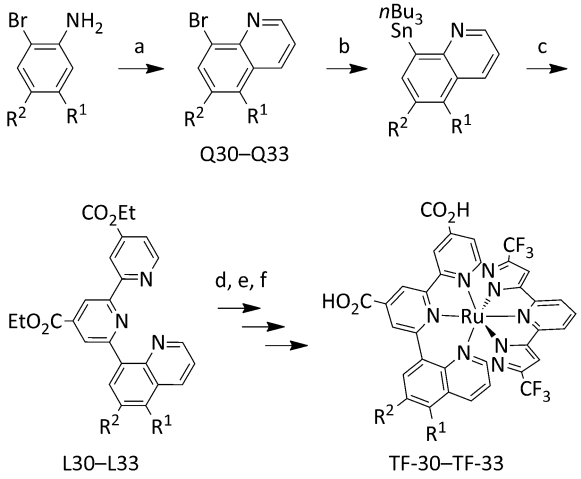

Scheme 2. TF-30: $R^1=H$; $R^2=CO_2H$, TF-31: $R^1=R^2=H$, TF-32: $R^1=H$; $R^2=t$Bu, TF-33: $R^1=t$Bu; $R^2=H$. Synthetic protocols: a) sodium *m*-nitrobenzenesulfonate, $FeSO_4\cdot 7H_2O$, glycerol, CH_3SO_3H, 135 °C; b) Sn_2nBu_6, $[PdCl_2(PPh_3)_2]$, toluene, reflux; c) diethyl 6-bromo-2,2′-bipyridine-4,4′-dicarboxylate, $[PdCl_2(PPh_3)_2]$, CuI, CsF, DMF, 110 °C; d) $RuCl_3\cdot 3H_2O$, EtOH, reflux; e) 2,6-bis(3-(trifluoromethyl)-5-pyrazolyl)pyridine, KOAc, toluene, reflux; f) 2 M NaOH, acetone, RT.

terpyridine anchor and derivatives[8] and hence to afford sensitizers with higher transition dipole moments, that is, absorptivity, for the corresponding π–π* and MLCT transitions. Chemically, the Qbpy anchors were also expected to be superior to bipyridine anchors with either carboxy-substituted alkenyl or thienyl appendages;[9] the latter lack the necessary rigidity to suppress the fast nonradiative deactivation pathways despite their lower-lying absorption band in the NIR region. Moreover, the nitrogen atoms of the terminal-pyridine and quinoline moieties of Qbpy were expected to align in a linear fashion to ensure a higher d–d excited-state energy (as in the case of terpyridine) and less quenching.[10] In fact, advances in 2,6-bis(8-quinolinyl)pyridine Ru^{II} complexes showed a record-breaking 3.0 μs lifetime for the emission at 700 nm at room temperature.[11] These factors support the use of Qbpy-type anchors for future high-performance ruthenium(II)-based sensitizers.

The targeted anchor required a key starting material, namely, functional 8-bromoquinolines Q30–Q33, which were prepared by the Skraup reaction.[12] These compounds were then converted into the corresponding tributylstannyl derivatives, which were treated with diethyl 6-bromo-2,2′-bipyridine-4,4′-dicarboxylate under Stille cross-coupling conditions to afforded the Qbpy anchors L30–L33 (Scheme 2). Next, the Ru^{II} complexes were obtained from the reaction of L30–L33 with $RuCl_3\cdot 3H_2O$, followed by treatment with 2,6-bis(3-trifluoromethyl-5-pyrazolyl)pyridine for incorporation of the ancillary chelating ligand. The crude ethoxycarbonyl Ru^{II} materials were then purified by column chromatography on silica gel. Finally, the ethoxycarbonyl groups were hydrolyzed in a mixture of acetone and a 2 M solution of NaOH at room temperature. The resulting Ru^{II} sensitizers TF-30–TF-33 were precipitated by adjusting the pH value of the solution to about pH 3, followed by rinsing with water and acetone, and drying in vacuo. Experimental details are provided in the Supporting Information.

The absorption spectra of reference sensitizer TF-1 and novel quinolinyl sensitizers TF-30–TF-33 in solution in DMF are depicted in Figure 1 together with that of black dye for a fair comparison. The pertinent numerical data for all samples are summarized in Table 1. These TF-3x dyes showed intense visible absorption bands down to 800 nm; the lower-energy bands were assigned to the metal-to-ligand charge transfer (MLCT) of the Qbpy anchor, together with a contribution from ligand-to-ligand charge transfer (LLCT) originating from the ancillary. Notably, the absorptions for the TF-3*x* sensitizers displayed the combined advantages of both black dye and TF-1, that is, much superior optical responses in the regime spanning the far-visible and NIR regions; such optical responses have never been documented for Ru^{II} sensitizers with the tctpy class of anchors.[8,13] The associated spectral assignment was further supported by theoretical calculations (see details in the Supporting Information and discussion below). Prominent NIR emission was observed for TF-3*x* sensitizers, with peak wavelengths at 820–850 nm. In this approach, a TF-3*x* concentration of less than 10^{-5} M was utilized to avoid intermolecular H bonding through carboxylic groups and/or π–π stacking between quinolinyl fragments (see below). The emission lifetimes of several tens of nanoseconds (Table 1), together with the favorable driving force, as supported by electrochemical measurements, ensure efficient electron injection into the TiO_2 electrode.

Cyclic voltammetry was conducted to ensure that the ground- and excited-state oxidation potentials ($E^{o\prime}$ and $E^{o\prime}$*) of the TF-3*x* sensitizers were more positive than the redox potential of the electrolyte (I^-/I_3^-: 0.4 V vs. NHE)[14] and more negative than the conduction-band potential of TiO_2 (ca. −0.5 V vs. NHE), respectively. The recorded $E^{o\prime}$ values appeared in the range 0.82–0.85 V (vs. NHE), whereas the $E^{o\prime}$* values were between −0.90 and −0.85 V (Table 1). These sets of values both fit the requirement for optimal device operation.

Table 1: Photophysical and electrochemical data for the studied TF-3*x* sensitizers.[a]

Dye	Abs. λ_{max} [nm] (ε [10^3 L mol^{-1} cm^{-1}])	λ_{em} [nm]	τ [ns]	$E^{0\prime}$ [V][b]	E_{0-0} [V][c]	$E^{0\prime *}$ [V][c]
black dye	398 (9.3), 525 (5.5), 599 (7.7)	806	94	0.88	1.67	−0.79
TF-30	404 (14), 523 (9.6), 656 (3.9)	823	31	0.85	1.70	−0.85
TF-31	403 (13), 521 (8.8), 653 (3.7)	840	22	0.83	1.70	−0.87
TF-32	404 (15), 519 (10), 647 (4.5)	835	105	0.82	1.72	−0.90
TF-33	402 (15), 516 (10), 650 (4.4)	842	32	0.82	1.71	−0.89

[a] Absorption spectra, emission peak maxima, and lifetime were measured in solution in DMF. [b] The oxidation potential of dyes was measured in DMF in the presence of $[Bu_4N][PF_6]$ (0.1 M) and with a scan rate of 50 mV s^{-1}. It was calibrated with Fc/Fc^+ as an internal reference and converted to the normal hydrogen electrode (NHE) by the addition of 0.63 V. [c] E_{0-0} was determined from the intersection of the absorption and tangent of the emission peak in DMF. $E^{0\prime *} = E^{0\prime} - E_{0-0}$.

the 450–700 nm region, owing to the difference between the Qbpy and terpyridine anchors. Time-dependent DFT (TD-DFT) calculations revealed that the lowest-lying HOMO→LUMO transition (in the singlet manifold) for TF-3*x* mainly involves Ru^{II}→Qbpy (MLCT) and 2,6-bis(pyrazolyl)pyridine→Qbpy (LLCT) transitions. However, except for partial involvement in TF-30, the quinolinyl moiety does not contribute significantly to this lowest-lying transition. Instead, the contribution of the quinolinyl moiety is ubiquitously seen in other higher-lying exited states between 500 and 700 nm for all of the TF-3*x* series (see Figure 3 for TF-30 and 32; see the Supporting Information for the other complexes). Thus, the extended π conjugation of Qbpy is the reason for the greater absorptivity of all TF-3*x* sensitizers as compared to TF-1 and related sensitizers.

As for TF-30, owing to the carboxylic substituent R^2 (Scheme 2), the lowering in energy and thus partial contribution to the LUMO of the quinolinyl moiety is expected. However, in contrast to the carboxylic groups in the pyridine moieties, the calculations for TF-30 revealed that the contribution of the R^2 carboxylic group to the LUMO is negligible (see Figure 3). Therefore, if two carboxylic groups are required for anchoring to the TiO_2 nanoparticles, as established for black dye,[16] statistically, half of the TF-30 units on TiO_2 should be anchored through the R^2 carboxylic group; furthermore, such an arrangement would suffer from a twisted configuration. Accordingly, the electron-coupling matrix is expected to be smaller, which offers one possible rationale for the inferior performance of TF-30. The lowered

The performance of these sensitizers was then examined in dye-sensitized solar cells (DSCs), the construction of which is detailed in the Supporting Information. The incident-photon-to-current conversion efficiencies (IPCEs) of these DSC devices are shown in Figure 2a, and the numerical data describing the performance of the DSCs are listed in Table 2. In sharp contrast to black dye with an IPCE onset at approximately 900 nm,[15] all recorded IPCE onsets of these TF-3x sensitizers were close to about 820 nm. The IPCE rose steeply to 80% at approximately 720 nm for TF-32 and TF-33, whereas the other TF-3x sensitizers showed notably inferior IPCE values under the same conditions. As evidenced by its absorption spectrum (Figure 1), TF-1 is hampered by its poor absorptivity relative to that of the investigated TF-3*x* series in

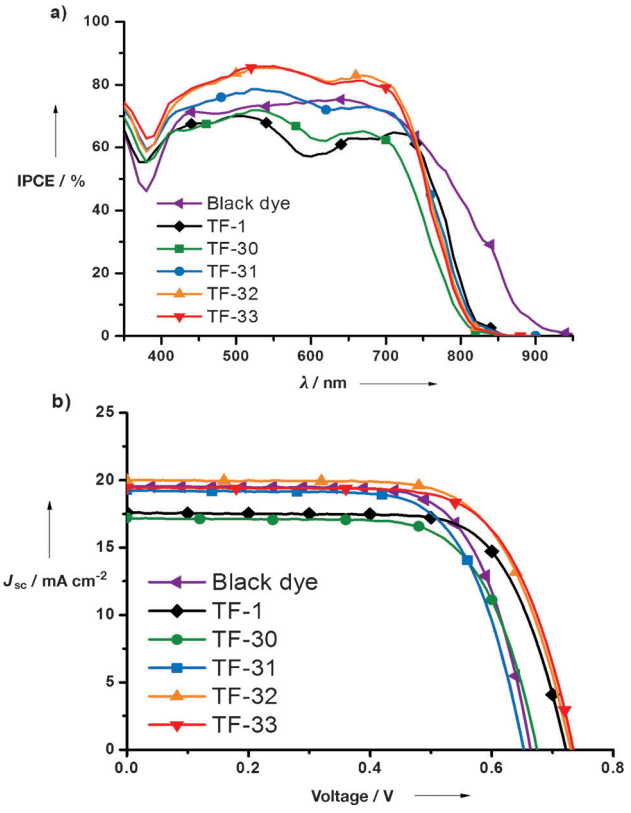

Figure 2. a) IPCE spectra and b) *J*–*V* characteristics measured for DSCs sensitized with various TF-3*x* sensitizers under AM1.5 solar irradiation.

Table 2: Performance of DSCs as measured under AM1.5 G simulated solar irradiation.[a]

Sensitizer	J_{SC} [mA cm^{-2}]	V_{OC} [V]	FF	η [%]	Dye loading[b] [10^{-7} mol cm^{-2}]
black dye	19.6	660	0.71	9.22	–
TF-1	17.6	720	0.72	9.15	2.01
TF-30	17.2	670	0.71	8.18	1.42
TF-31	19.3	650	0.70	8.76	1.63
TF-32	19.2	740	0.72	10.19	1.23
TF-33	19.4	730	0.71	10.04	1.44

[a] All devices were fabricated with (15 + 7) μm TiO_2 anodes and with a projected area of 5 × 5 mm^2. The dye (0.3 mM) was dissolved in absolute ethanol and *t*BuOH (v/v, 1:1) with tetrabutylammonium deoxycholate [TBA][DOC] (2 equiv). The device performance was measured by using a black metal mask with a square aperture of size 4 × 4 mm^2. The electrolyte consisted of DMPII (1,2-dimethyl-3-propylimidazolium iodide) (0.6 M), LiI (0.05 M), I_2 (0.05 M), and tBP (4-*tert*-butylpyridine) (0.5 M) in acetonitrile. [b] The value was calculated from the MLCT band ratio for the solution of the desorbed dye versus a 0.01 mM reference solution in mixed MeOH and water (v/v, 1:1) in the presence of [TBA]OH (0.1 M).

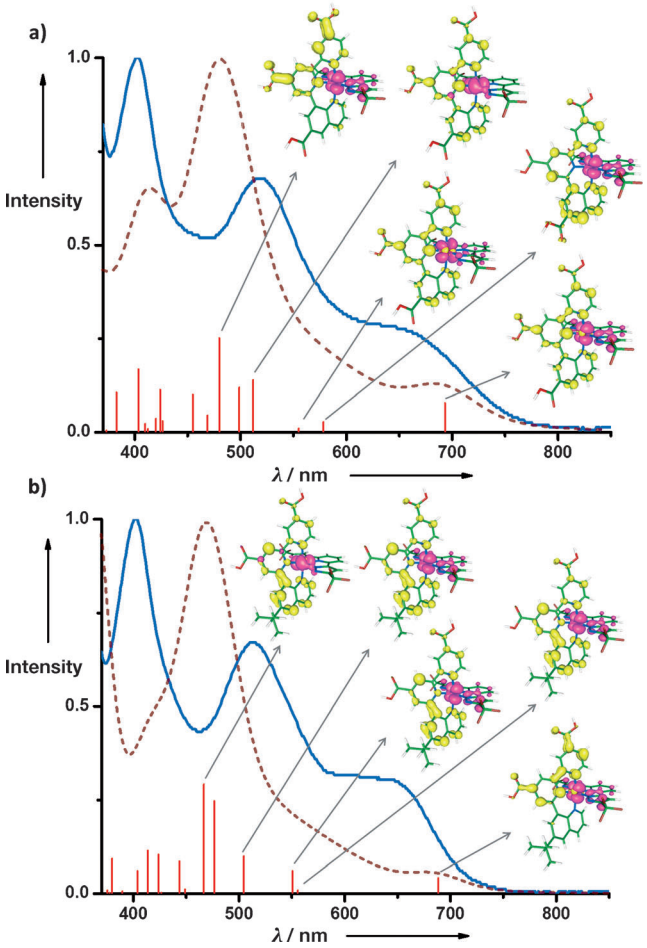

Figure 3. Experimental (solid line) and TD-DFT calculated (dashed line obtained with a Gaussian convolution with $\sigma = 0.2$ eV) absorption spectra of sensitizers im DMF: a) TF-30 and b) TF-32. Also depicted are the TD-DFT calculated absorption wavelengths (vertical lines) and the relative transition probability (magnitude of vertical lines). Selected frontier orbitals (pink: occupied orbital, yellow: unoccupied orbital) that contribute to the major transitions are also shown.

IPCE of TF-31, from a structural point of view, could be due to unwanted intermolecular π–π stacking between the quinolinyl substituents. Support for this hypothesis was obtained by single-crystal X-ray structural analysis of the esterified derivative TF-31Et, for which an interplanar contact of 3.298 Å between the quinolinyl fragments was estimated (see Figures S3 and S4 in the Supporting Information). Therefore, the interaction of TF-31 with the TiO_2 surface might hamper somewhat the electron injection. Conversely, the bulky *tert*-butyl substituents in both TF-32 and TF-33 inhibit this intermolecular stacking and provide a higher IPCE, as observed.

Figure 2b shows the photocurrent-density–voltage curves recorded for the DSC devices under simulated sunlight (AM1.5 G) at a light intensity of 100 mW cm^{-2}. The sensitizers TF-32 and TF-33 showed the best set of data among all the sensitizers tested. Although the conversion efficiencies of TF-32 and TF-33 ($\eta = 10.19$ and 10.04%) are slightly lower than that of the best DSC performance recorded for cosensitized black dye (certified: 11.4%; uncertified: 11.8%)[17] and for C106 (uncertified: 11.7%),[18] our data are outstanding as they show a trend upon systematic changes to the TF-3*x* structure. Moreover, the *tert*-butyl group accomplished its intended function of suppressing the dark current[19] to give the highest observed V_{OC} value (740 mV) for the present system. The slightly lower J_{SC} value of 19.2 mA cm^{-2} for TF-32 relative to 19.4 mA cm^{-2} for TF-33 could be due to a positional effect of the *tert*-butyl group, but the exact cause remains unclear at this time.

Charge-transfer processes in these devices were investigated on the basis of transient spectroscopic measurements. To help us understand the factors that affect the observed V_{OC} value, we conducted charge-extraction and transient-photovoltage (TPV) measurements.[20] Charge-extraction experiments indicated similar TiO_2 conduction-band edges for all devices except for TF-31 (Figure 4). This difference can be understood in terms of more adsorption of the tBP additive on the TiO_2 surface in the case of TF-31.[21] Among the sensitizers, TF-31 is anchored through the least bulky Qbpy chelate. Therefore, the intermolecular π–π stacking between the quinolinyl substituents (see above) induces packing and hence congestion of TF-31 on the TiO_2 surface. The net result may be the creation of a larger void/extra space

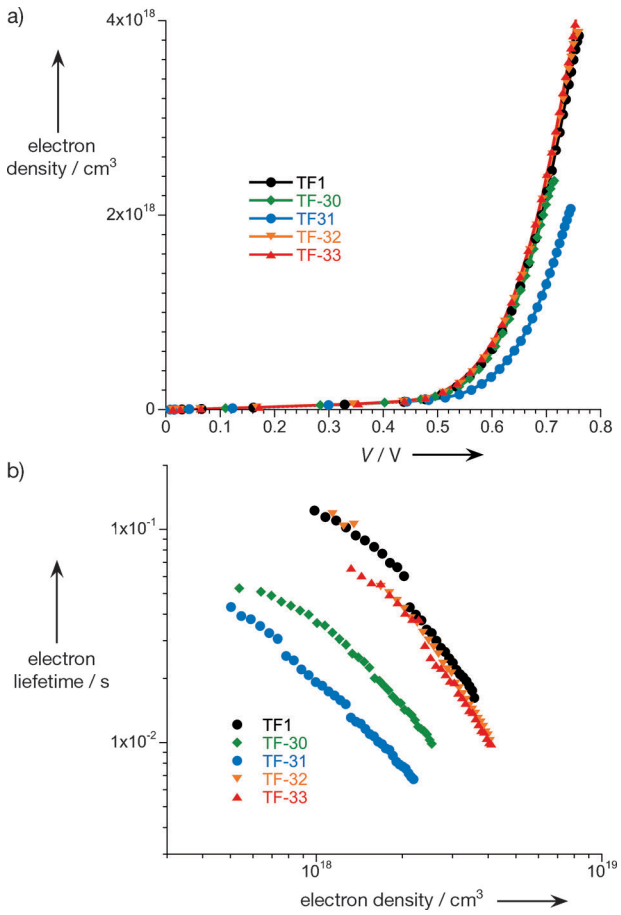

Figure 4. a) TiO_2 electron density versus voltage deduced from charge-extraction measurements and b) electron lifetime τ versus TiO_2 electron density deduced from transient photovoltage measurements for DSC devices containing TF sensitizers.

in TiO_2 to facilitate tBP access to the TiO_2 surface, thus raising the tail of the conduction band in the TF-31 device. Transient photovoltage data subsequently showed that TF-1, TF-32, and TF-33 have almost identical electron lifetimes, and this characteristic coupled to the similar electron densities explains their higher V_{OC} values of 720–730 mV. Moreover, the electron lifetimes show the blocking effect of the bulky *tert*-butyl substituents on TF-32 and TF-33. Although the TF-31 device has the shortest electron lifetime owing to the fastest charge recombination, the fact that its conduction band edge is shifted further upwards as compared to the other devices explains why its V_{OC} value is comparable to that of the TF-30 device with its longer electron lifetime. Transient absorption measurements were used to measure regeneration in TF-3*x* devices by the I^-/I_3^- electrolyte. The regeneration half-life ($t_{50\%}$) was found to be almost exactly the same for all devices (70–80 μs; see the Supporting Information), which is consistent with the similar ground-state oxidation potential for all dyes in the series.

Finally, the device stability of TF-3*x* sensitizers was investigated. In this study, the lifespan of solar cells fabricated with TF-32 on a $(15+7)$ μm TiO_2 electrode was carefully examined by long-term accelerated aging under accelerated visible-light soaking at 60 °C. After illumination for 1000 h, the efficiency changed only slightly: The J_{SC} value changed from 17.6 to 17.8 mA cm^{-2}, the V_{OC} value from 720 to 690 mV, the fill factor (FF) from 0.67 to 0.71, and the η value from 8.51 to 8.75 % (see Figure S9). This stability indicates the practical advantage of Ru^{II} sensitizers with this new class of Qbpy anchor.

In conclusion, we have strategically designed and synthesized a series of Ru^{II} sensitizers bearing novel Qbpy tridentate anchors. Qbpy offers never before reported advantages over the existing tctpy anchor of black dye. The elongation of the quinoline π conjugation greatly increases the absorptivity at higher-lying states covering the visible to NIR regions; on the other hand, the structural rigidity partially inhibits the nonradiative deactivation of the sensitizer and allows for rapid electron injection. These characteristics, in combination with the 2,6-bis(pyrazolyl)pyridine ancillary, establish a bis-(tridentate) Ru^{II} motif with superior structural stability and panchromatic absorptivity. A DSC device based on the representative sensitizer TF-32 afforded a remarkable DSC performance of $J_{SC} = 19.2$ mA cm^{-2}, $V_{OC} = 740$ mV, FF = 0.72, and $\eta = 10.19\,\%$. Thus, this Qbpy anchor could be utilized to replace the tctpy anchor of black dye[2a] and/or to derivatize the recently reported triplet Ru^{II} sensitizers featuring the same tctpy anchor and coordinated phosphines.[22]

Received: July 10, 2013
Revised: September 27, 2013
Published online: November 11, 2013

Keywords: N ligands · panchromatic sensitizers · quinolines · ruthenium · solar cells

[1] a) M. Grätzel, *Acc. Chem. Res.* **2009**, *42*, 1788; b) A. Hagfeldt, G. Boschloo, L. Sun, L. Kloo, H. Pettersson, *Chem. Rev.* **2010**, *110*, 6595; c) P. K. Nayak, J. Bisquert, D. Cahen, *Adv. Mater.* **2011**, *23*, 2870; d) C. Grätzel, S. M. Zakeeruddin, *Mater. Today* **2013**, *16*, 11.

[2] a) M. K. Nazeeruddin, P. Péchy, T. Renouard, S. M. Zakeeruddin, R. Humphry-Baker, P. Comte, P. Liska, L. Cevey, E. Costa, V. Shklover, L. Spiccia, G. B. Deacon, C. A. Bignozzi, M. Grätzel, *J. Am. Chem. Soc.* **2001**, *123*, 1613; b) M. Grätzel, *Inorg. Chem.* **2005**, *44*, 6841.

[3] a) P. Wang, S. M. Zakeeruddin, J. E. Moser, M. K. Nazeeruddin, T. Sekiguchi, M. Grätzel, *Nat. Mater.* **2003**, *2*, 402; b) C.-Y. Chen, M. Wang, J.-Y. Li, N. Pootrakulchote, L. Alibabaei, C.-H. Ngoc-Le, J.-D. Decoppet, J.-H. Tsai, C. Grätzel, C.-G. Wu, S. M. Zakeeruddin, M. Grätzel, *ACS Nano* **2009**, *3*, 3103; c) Y. Cao, Y. Bai, Q. Yu, Y. Cheng, S. Liu, D. Shi, F. Gao, P. Wang, *J. Phys. Chem. C* **2009**, *113*, 6290; d) S.-W. Wang, K.-L. Wu, E. Ghadiri, M. G. Lobello, S.-T. Ho, Y. Chi, J.-E. Moser, F. De Angelis, M. Grätzel, M. K. Nazeeruddin, *Chem. Sci.* **2013**, *4*, 2423.

[4] a) S. Zhang, X. Yang, Y. Numata, L. Han, *Energy Environ. Sci.* **2013**, *6*, 1443; b) Y. Wu, W. Zhu, *Chem. Soc. Rev.* **2013**, *42*, 2039; c) Y.-S. Yen, H.-H. Chou, Y.-C. Chen, C.-Y. Hsu, J. T. Lin, *J. Mater. Chem.* **2012**, *22*, 8734; d) Y. Ooyama, Y. Harima, *ChemPhysChem* **2012**, *13*, 4032; e) P. G. Bomben, K. C. D. Robson, B. D. Koivisto, C. P. Berlinguette, *Coord. Chem. Rev.* **2012**, *256*, 1438; f) J. N. Clifford, E. Martínez-Ferrero, A. Viterisi, E. Palomares, *Chem. Soc. Rev.* **2011**, *40*, 1635; g) Z. Ning, Y. Fu, H. Tian, *Energy Environ. Sci.* **2010**, *3*, 1170.

[5] H. J. Snaith, *Adv. Funct. Mater.* **2010**, *20*, 13.

[6] Z.-S. Wang, H. Kawauchi, T. Kashima, H. Arakawa, *Coord. Chem. Rev.* **2004**, *248*, 1381.

[7] C.-C. Chou, K.-L. Wu, Y. Chi, W.-P. Hu, S. J. Yu, G.-H. Lee, C.-L. Lin, P.-T. Chou, *Angew. Chem.* **2011**, *123*, 2102; *Angew. Chem. Int. Ed.* **2011**, *50*, 2054.

[8] a) S.-H. Yang, K.-L. Wu, Y. Chi, Y.-M. Cheng, P.-T. Chou, *Angew. Chem.* **2011**, *123*, 8420; *Angew. Chem. Int. Ed.* **2011**, *50*, 8270; b) K.-L. Wu, C.-H. Li, Y. Chi, J. N. Clifford, L. Cabau, E. Palomares, Y.-M. Cheng, H.-A. Pan, P.-T. Chou, *J. Am. Chem. Soc.* **2012**, *134*, 7488; c) M. Kimura, H. Nomoto, N. Masaki, S. Mori, *Angew. Chem.* **2012**, *124*, 4447; *Angew. Chem. Int. Ed.* **2012**, *51*, 4371; d) M. Kimura, J. Masuo, Y. Tohata, K. Obuchi, N. Masaki, T. N. Murakami, N. Koumura, K. Hara, A. Fukui, R. Yamanaka, S. Mori, *Chem. Eur. J.* **2013**, *19*, 1028; e) Y. Numata, S. P. Singh, A. Islam, M. Iwamura, A. Imai, K. Nozaki, L. Han, *Adv. Funct. Mater.* **2013**, *23*, 1817.

[9] a) S.-R. Jang, J.-H. Yum, C. Klein, K.-J. Kim, P. Wagner, D. Officer, M. Grätzel, M. K. Nazeeruddin, *J. Phys. Chem. C* **2009**, *113*, 1998; b) A. Mishra, N. Pootrakulchote, M. K. R. Fischer, C. Klein, M. K. Nazeeruddin, S. M. Zakeeruddin, P. Bäuerle, M. Grätzel, *Chem. Commun.* **2009**, 7146; c) A. Mishra, N. Pootrakulchote, M. Wang, S.-J. Moon, S. M. Zakeeruddin, M. Grätzel, P. Bäuerle, *Adv. Funct. Mater.* **2011**, *21*, 963; d) K.-L. Wu, W.-P. Ku, S.-W. Wang, A. Yella, Y. Chi, S.-H. Liu, P.-T. Chou, M. K. Nazeeruddin, M. Grätzel, *Adv. Funct. Mater.* **2013**, *23*, 2285.

[10] M. Abrahamsson, H. Wolpher, O. Johansson, J. Larsson, M. Kritikos, L. Eriksson, P.-O. Norrby, J. Bergquist, L. Sun, B. Aakermark, L. Hammarström, *Inorg. Chem.* **2005**, *44*, 3215.

[11] a) M. Abrahamsson, M. Jäger, T. Österman, L. Eriksson, P. Persson, H.-C. Becker, O. Johansson, L. Hammarström, *J. Am. Chem. Soc.* **2006**, *128*, 12616; b) M. Abrahamsson, M. Jäger, R. J. Kumar, T. Österman, P. Persson, H.-C. Becker, O. Johansson, L. Hammarström, *J. Am. Chem. Soc.* **2008**, *130*, 15533.

[12] D. A. Conlon, A. Drahus-Paone, G.-J. Ho, B. Pipik, R. Helmy, J. M. McNamara, Y.-J. Shi, J. M. Williams, D. Macdonald, D. Deschenes, M. Gallant, A. Mastracchio, B. Roy, J. Scheigetz, *Org. Process Res. Dev.* **2006**, *10*, 36.

[13] a) B.-S. Chen, K. Chen, Y.-H. Hong, W.-H. Liu, T.-H. Li, C.-H. Lai, P.-T. Chou, Y. Chi, G.-H. Lee, *Chem. Commun.* **2009**, 5844; b) T. Funaki, H. Funakoshi, O. Kitao, N. Onozawa-Komatsuzaki,

K. Kasuga, K. Sayama, H. Sugihara, *Angew. Chem.* **2012**, *124*, 7646; *Angew. Chem. Int. Ed.* **2012**, *51*, 7528.
[14] a) S. Ardo, G. J. Meyer, *Chem. Soc. Rev.* **2009**, *38*, 115; b) G. Boschloo, E. A. Gibson, A. Hagfeldt, *J. Phys. Chem. Lett.* **2011**, *2*, 3016.
[15] Y. Chiba, A. Islam, Y. Watanabe, R. Komiya, N. Koide, L. Han, *Jpn. J. Appl. Phys.* **2006**, *45*, L638.
[16] S.-H. Liu, H. Fu, Y.-M. Cheng, K.-L. Wu, S.-T. Ho, Y. Chi, P.-T. Chou, *J. Phys. Chem. C* **2012**, *116*, 16338.
[17] a) L. Han, A. Islam, H. Chen, C. Malapaka, B. Chiranjeevi, S. Zhang, X. Yang, M. Yanagida, *Energy Environ. Sci.* **2012**, *5*, 6057; b) H. Ozawa, R. Shimizu, H. Arakawa, *RSC Adv.* **2012**, *2*, 3198; c) H. Ozawa, Y. Okuyama, H. Arakawa, *RSC Adv.* **2013**, *3*, 9175.
[18] Q. Yu, Y. Wang, Z. Yi, N. Zu, J. Zhang, M. Zhang, P. Wang, *ACS Nano* **2010**, *4*, 6032.
[19] a) M. García-Iglesias, L. Pellejà, J.-H. Yum, D. González-Rodriguez, M. K. Nazeeruddin, M. Grätzel, J. N. Clifford, E. Palomares, P. Vázquez, T. Torres, *Chem. Sci.* **2012**, *3*, 1177; b) K.-L. Wu, W.-P. Ku, J. N. Clifford, E. Palomares, S.-T. Ho, Y. Chi, S.-H. Liu, P.-T. Chou, M. K. Nazeeruddin, M. Grätzel, *Energy Environ. Sci.* **2013**, *6*, 859.
[20] a) D. Credgington, J. R. Durrant, *J. Phys. Chem. Lett.* **2012**, *3*, 1465; b) P. R. F. Barnes, K. Miettunen, X. Li, A. Y. Anderson, T. Bessho, M. Grätzel, B. C. O'Regan, *Adv. Mater.* **2013**, *25*, 1881.
[21] a) G. Schlichthörl, S. Y. Huang, J. Sprague, A. J. Frank, *J. Phys. Chem. B* **1997**, *101*, 8141; b) S. Nakade, T. Kanzaki, W. Kubo, T. Kitamura, Y. Wada, S. Yanagida, *J. Phys. Chem. B* **2005**, *109*, 3480; c) S. E. Koops, B. C. O'Regan, P. R. F. Barnes, J. R. Durrant, *J. Am. Chem. Soc.* **2009**, *131*, 4808.
[22] T. Kinoshita, J. T. Dy, S. Uchida, T. Kubo, H. Segawa, *Nat. Photonics* **2013**, *7*, 535.

